

1  
2  
3  
4  
5  
6  
7  
8  
9  
10  
11  
12  
13  
14  
15  
16  
17  
18

Trogocytosis by *Entamoeba histolytica* mediates acquisition and display of human cell  
membrane proteins and evasion of lysis by human serum

Hannah W. Miller<sup>1</sup>, Rene L. Suleiman<sup>1</sup> and Katherine S. Ralston<sup>1\*</sup>

<sup>1</sup>Department of Microbiology and Molecular Genetics, University of California, Davis, California, United  
States of America

\*Corresponding author

E-mail: ksralston@ucdavis.edu (KR)

## 19 **Abstract**

20  
21 *Entamoeba histolytica* is the protozoan parasite responsible for amoebiasis. We previously showed  
22 that *E. histolytica* kills human cells through a mechanism that we termed trogocytosis (*trogo-*: nibble), due to  
23 its resemblance to trogocytosis in other organisms. In parasites, trogocytosis is used to kill host cells. In  
24 multicellular organisms, trogocytosis is used for cell-cell interactions in the immune system, in the central  
25 nervous system, and during development. Thus, nibbling is an emerging theme in cell-cell interactions both  
26 within and between species, and it is relevant to host-pathogen interactions in many different contexts. When  
27 trogocytosis occurs between mammalian immune cells, cell membrane proteins from the nibbled cell can be  
28 acquired and displayed by the recipient cell. In this study, we tested the hypothesis that through trogocytosis  
29 of human cells, amoebae acquire and display human cell membrane proteins. Here we demonstrate for the  
30 first time that through trogocytosis, *E. histolytica* acquires and displays human cell membrane proteins and  
31 that this leads to protection from lysis by human serum. Protection from human serum only occurs after  
32 amoebae have undergone trogocytosis of live cells, but not phagocytosis of dead cells. Likewise, mutant  
33 amoebae that exhibit a phagocytosis defect, but are unaltered in their capacity to perform trogocytosis, are  
34 nevertheless protected from human serum. Our studies are the first to demonstrate that amoebae can display  
35 human cell membrane proteins and suggest that acquisition and display of membrane proteins is a general  
36 feature of trogocytosis that is not restricted to trogocytosis between mammalian immune cells. These studies  
37 have major implications for interactions between *E. histolytica* and the immune system and also reveal a novel  
38 strategy for immune evasion by a pathogen. Since other microbial eukaryotes use trogocytosis for cell killing,  
39 our findings may apply to the pathogenesis of other infections.

## 40 Author Summary

41 *Entamoeba histolytica* is an intestinal parasite that causes amoebiasis, a potentially fatal diarrheal  
42 disease. Abscesses in organs outside of the intestine, such as the liver, can occur when amoebae are able to  
43 breach the intestinal wall and travel through the blood stream to other areas of the body. We previously  
44 showed that *E. histolytica* kills human cells by taking “bites” of human cell material in a process that we  
45 named trogocytosis (*trogo*-: nibble). Mammalian immune cells use trogocytosis to acquire proteins from other  
46 cells which impacts cell-cell communication. Here we tested the hypothesis that trogocytosis allows *E.*  
47 *histolytica* to acquire and display proteins from human cells allowing amoebae to survive in the blood stream.  
48 We demonstrate for the first time that through trogocytosis, *E. histolytica* acquires and displays human cell  
49 membrane proteins. We also demonstrate that trogocytosis of human cells allows amoebae to survive in  
50 human serum. These studies reveal a novel strategy for immune evasion by a pathogen and may apply to the  
51 pathogenesis of other infections.

## 52 Introduction

53

54 *Entamoeba histolytica* is the protozoan parasite responsible for amoebiasis, a potentially fatal diarrheal  
55 disease. Amoebiasis occurs worldwide and is most prevalent in developing countries, in areas with poor  
56 sanitation and high malnutrition [1–3]. For instance, a recent study found that nearly 80% of infants living in  
57 an urban slum in Bangladesh had been infected with *E. histolytica* by two years of age [4]. The infection has a  
58 wide range of clinical symptoms that include asymptomatic infection, diarrhea, bloody diarrhea, and fatal  
59 abscesses outside of the intestine. Bloody diarrhea arises when amoebic trophozoites (amoebae) invade and  
60 ulcerate the intestine. Amoebae that have invaded the intestine can then disseminate and cause abscesses in  
61 other tissues, most commonly in the liver. Although amoebic liver abscesses are rare, they are fatal if  
62 untreated. Little is known about the mechanisms that allow *E. histolytica* to evade immune detection and  
63 disseminate upon entering the bloodstream during invasive amoebiasis.

64 The parasite was named “histolytica” for its ability to damage tissue (*histo-*: tissue; *lytic-*: dissolving)  
65 [5–7]. Despite this name-giving property, how amoebae invade and damage tissues is not clear. The most well-  
66 known virulence factor is the amoeba surface D-galactose and N-acetyl-D-galactosamine (Gal/GalNAc) lectin  
67 [8,9], which mediates attachment to human cells and intestinal mucin [10–13]. Surface-localized and secreted  
68 cysteine proteases contribute to proteolysis of human substrates including mucin and extracellular matrix [10–  
69 13]. The profound cell killing activity of amoebae is likely to drive tissue damage. Amoebae can kill almost any  
70 type of human cell within minutes and direct contact with human cells is required for killing to occur [8,9].  
71 Until recently, the accepted model was that the pore-forming amoebapores act as secreted toxins [14–17].  
72 However, the contact-dependence of cell killing [8,9], and the lack of killing activity in cell lysates and  
73 supernatants [6,7,18], are not consistent with the presence of secreted toxins. Furthermore, transfer of  
74 amoebapores to human cells has not been demonstrated.

75 We previously established a new paradigm by showing that *E. histolytica* kills human cells through a  
76 mechanism that we termed trogocytosis (*trogo*-: nibble), due to its resemblance to trogocytosis in other  
77 organisms [19]. During trogocytosis, amoebae kill human cells by extracting and ingesting “bites” of human  
78 cell membrane and intracellular contents [19]. We defined that trogocytosis requires amoebic actin  
79 rearrangements [19]. It also requires signaling initiated by the Gal/GalNAc lectin, phosphatidylinositol 3-  
80 kinase (PI3K) signaling and an amoebic C2 domain-containing kinase (*EhC2PK*) [19]. By applying multiphoton  
81 imaging using explanted mouse intestinal tissue from fluorescent-membrane mice, we found that trogocytosis  
82 was required for tissue invasion, demonstrating relevance to pathogenesis [19].

83 Trogocytosis is not specific to *E. histolytica*, as it can be observed in other microbial eukaryotes as well  
84 as multicellular eukaryotes [20]. Examples in microbes include reports of trogocytosis by *Naegleria fowleri* [21]  
85 and by *Dictyostelium caveatum* [22]. In multicellular eukaryotes, trogocytosis is used for cell-cell  
86 communication and cell-cell remodeling. Trogocytosis plays roles in the immune system [23,24], in the central  
87 nervous system [25,26], and during development [27]. Additionally, intracellular bacteria exploit macrophage  
88 trogocytosis to spread from cell to cell [28]. It is not yet clear how trogocytosis can paradoxically be both a  
89 benign form of cell-cell interaction and a mechanism for cell-killing. The previous paradigm was that microbes  
90 engage trogocytosis for cell-killing, but trogocytosis in multicellular organisms was believed to be a benign  
91 form of cell-cell interaction. However, recent reports have now shown that neutrophils can use trogocytosis to  
92 kill parasites [29], and that neutrophils and macrophages can use trogocytosis to kill cancer cells in a form of  
93 antibody-dependent cell-mediated cytotoxicity [30,31]. Trogocytosis is therefore likely to be a conserved,  
94 fundamental form of eukaryotic cell-cell interaction that can be cytotoxic or benign, depending on the context.

95 One intriguing outcome of trogocytosis between mammalian immune cells is that it changes the  
96 makeup of cell surface proteins on both the donor and the recipient cell. The nibbling cell is able to display the  
97 acquired membrane proteins from the nibbled cell on its surface [24,32]. Acquired membrane proteins appear  
98 as foci or patches on the recipient cell. This allows the recipient cell to take on new properties that impact its

99 subsequent interactions with other cells [24,32]. For instance, uninfected dendritic cells can acquire and  
100 display pre-loaded major histocompatibility complex class II (MHC II) molecules by nibbling infected dendritic  
101 cells, and thus they can present peptides from microbes they have not directly encountered, which has been  
102 termed “cross-dressing” [24]. Transferred molecules are not limited to MHC complexes as induced regulatory  
103 T cells can acquire cluster of differentiation (CD) molecules from mature dendritic cells including CD80 and  
104 CD86 [33]. It has also been shown that monocytes, NK cells, and granulocytes can acquire CD22, CD19, CD21,  
105 and CD79b from antibody-opsonized B cells [34]. In addition to allowing the nibbling cell to display newly  
106 acquired membrane proteins, trogocytosis also affects the makeup of surface proteins on the nibbled cell.  
107 Since membrane fragments are removed from the nibbled cell, trogocytosis affects the nibbled cell by  
108 effectively downregulating surface proteins [35].

109         Since mammalian immune cells acquire and display membrane proteins through trogocytosis, we  
110 hypothesized that amoebae may acquire and display human cell membrane proteins during trogocytosis.  
111 Amoebic display of human proteins would have significant implications for host-pathogen interactions. We  
112 predicted that one outcome of amoebic human cell protein display could be the inhibition of lysis by human  
113 complement. Previous studies have suggested that amoebae become more resistant to complement after  
114 interacting with host cells or tissues, and that complement resistance involves proteins on the amoeba  
115 surface. For example, amoebae became more resistant to complement after co-incubation with erythrocytes,  
116 and an antibody directed towards an erythrocyte membrane protein reacted with the amoeba surface after  
117 erythrocyte co-incubation [36]. Animal-passaged amoebae are more resistant to complement lysis than  
118 control amoebae [37], and treatment of complement-resistant amoebae with trypsin renders amoebae  
119 complement-sensitive [38].

120         Here we show that *E. histolytica* acquires and displays human cell membrane proteins. Acquisition and  
121 display of human cell membrane proteins requires actin and is associated with subsequent protection from  
122 lysis by human serum. Protection from human serum further requires actin and direct contact between

123 amoebae and human cells. Protection from human serum occurs after amoebae have undergone trogocytosis,  
124 but not phagocytosis, suggesting protection is not generally associated with ingestion. Furthermore, mutant  
125 amoebae that are deficient in performing phagocytosis but not trogocytosis are still protected from human  
126 serum. Collectively, these findings support that amoebae acquire and display human cell membrane proteins  
127 through trogocytosis and that this leads to protection from lysis by human serum complement. These studies  
128 have major implications for interactions between *E. histolytica* and the immune system. Display of human cell  
129 proteins acquired during trogocytosis is a novel strategy for immune evasion by a pathogen. Since other  
130 microbial eukaryotes use trogocytosis for cell killing, this may apply to the pathogenesis of other infections.

## 131 Results

### 133 Amoebae acquire and display human cell membrane proteins

134 We first asked whether trogocytosis by *E. histolytica* could result in transfer of human cell membrane  
135 proteins to the cell membrane of the amoeba. Human Jurkat T cells were surface-biotinylated and then co-  
136 incubated with amoebae. After co-incubation, cells were fixed and labeled with fluorescently-conjugated  
137 streptavidin (Fig 1A). Since cells were not permeabilized, this approach required human cell proteins to be  
138 surface-exposed and to retain correct orientation. After five minutes of co-incubation, patches of streptavidin-  
139 labeled human cell proteins were detected on the surface of amoebae (Fig 1B – 1C, arrows). Similar to  
140 immune cell “cross-dressing” [24], the biotin-streptavidin label appeared as patches or foci on the amoeba  
141 surface. To track an individual human cell membrane protein, immunofluorescence was used to detect human  
142 major histocompatibility complex class I (MHC I) (Fig 1D). Following co-incubation, cells were fixed without  
143 permeabilization, and MHC I was detected using a monoclonal antibody. Comparable to the biotin-  
144 streptavidin labeling experiments, MHC I was detected in patches on the surface of amoebae after five  
145 minutes of co-incubation (Fig 1E – 1F). Together, these results suggested that human cell membrane proteins  
146 were acquired and displayed by amoebae following co-incubation with live human cells.  
147

### 148 Acquisition and display of human cell membrane proteins requires actin

149 Trogocytosis by *E. histolytica* requires actin rearrangements and is inhibited by treatment with  
150 cytochalasin D [19]. Therefore, we next asked whether transfer of human cell membrane proteins required  
151 actin. Imaging flow cytometry was used to quantitatively analyze displayed biotinylated human cell membrane  
152 proteins on the amoeba surface. It was important to distinguish between amoebae that displayed human cell  
153 membrane proteins and amoebae that were attached to intact, extracellular human cells. While the latter may  
154 also display human cell membrane proteins, we focused our analysis on images that lacked extracellular  
155 human cells as this allowed for the highest stringency in quantifying displayed human cell membrane proteins.

156 Since human cell nuclei are not internalized by amoebae during trogocytosis [19], human cell nuclei were  
157 fluorescently labeled, and this was used to gate images that contained or lacked extracellular human cells.

158 Human cell nuclei were labeled with Hoechst, and human cell membrane proteins were biotinylated  
159 prior to co-incubation with CellTracker Green CMFDA Dye (CMFDA)-labeled amoebae. After gating on single  
160 amoebae out of total cells (Fig 2A, S1 Fig), Hoechst staining was used to gate on images of amoebae with and  
161 without extracellular human cells (Fig 2B, D, F). Next, the extent of overlap of fluorescent-streptavidin and  
162 individual amoebae was quantified (Fig 2C, E). In the dimethyl sulfoxide (DMSO) treated control amoebae,  
163 25% of amoebae contained patches of biotin labeling (Human Cell Nuclei-/Biotin+), while in the cytochalasin D  
164 treated amoebae, 5% of amoebae contained patches of biotin labeling (Fig 2E). From this, we concluded that  
165 amoebae acquire and display human cell membrane proteins through an actin-dependent process, consistent  
166 with trogocytosis.

### 167 **Interaction with human cells leads to protection from lysis by human serum**

168 The acquisition and display of human cell membrane proteins has many potential implications for host-  
169 parasite interactions. One possible implication is in resistance to lysis by complement in human serum,  
170 particularly since it has been previously suggested that ingestion of human erythrocytes protects amoebae  
171 from lysis by human complement [36]. Amoebae preferentially perform trogocytosis on live human cells [19],  
172 therefore amoebae were incubated in the presence or absence of live human cells and then exposed to  
173 human serum (Fig 3A, S2 Fig). Using imaging flow cytometry, amoeba viability (Fig 3C – D), and trogocytosis  
174 were simultaneously measured (Fig 3B, S3 Fig). Amoebae that had interacted with live human cells, and had  
175 thus undergone trogocytosis and acquired human cell membrane proteins, were quantitatively protected from  
176 lysis by human serum (Fig 3C – 3D, S4 Fig). Among amoebae that had been incubated with human cells,  
177 amoebae that were lysed by human serum had generally undergone less trogocytosis than amoebae that

178 survived exposure to human serum (Fig 3E). Therefore, trogocytosis is associated with subsequent protection  
179 from lysis by human serum.

### 180 **Protection from human serum lysis is dependent on contact with human cells**

181 We next asked if protection from serum lysis required direct contact between amoebae and human  
182 cells, in order to determine if protection is a consequence of trogocytosis, or if protection could be acquired  
183 through secretion of proteins or release of exosomes by human cells. Amoebae and human cells were co-  
184 incubated in transwell dishes, with or without direct contact (Fig 4A). After incubation, cells from the lower  
185 chambers were exposed to human serum and imaging flow cytometry was used to measure amoeba viability.  
186 Human cells were not able to pass through transwell membranes (Fig 4B). Protection from complement lysis  
187 occurred only when amoebae and human cells were incubated together in the same chamber of the transwell,  
188 but not when they were separated (Fig 4C). Protection from human serum thus required direct contact  
189 between amoebae and human cells, supporting a requirement for trogocytosis in the acquisition of  
190 protection.

### 191 **Protection from human serum requires actin**

192 Since amoebic trogocytosis requires actin rearrangement [19], and acquisition and display of human  
193 cell membrane proteins requires actin (Fig 2), we next asked if treatment with cytochalasin D would also  
194 abrogate protection from human serum. Amoebae were treated with cytochalasin D, incubated in the  
195 presence or absence of human cells, and then exposed to human serum. Imaging flow cytometry was used to  
196 simultaneously measure trogocytosis (Fig 5A) and amoeba viability (Fig 5B). Amoebae that were treated with  
197 cytochalasin D were impaired in their ability to undergo trogocytosis and were not protected from serum lysis  
198 after co-incubation with human cells. Actin rearrangements are thus required for subsequent protection from  
199 lysis by human serum.

### 200 **Protection occurs after trogocytosis and does not occur after phagocytosis**

201 To ask if protection from human serum specifically occurs after trogocytosis, or if any form of ingestion  
202 leads to protection from serum, we compared amoebae that had undergone trogocytosis versus those that  
203 had undergone phagocytosis. We previously showed that amoebae undergo trogocytosis of live human cells,  
204 and in contrast, undergo phagocytosis of pre-killed human cells [19]. Therefore, we asked if phagocytosis of  
205 pre-killed cells could also provide protection from complement lysis. Human cells were pretreated with  
206 staurosporine to induce apoptosis (Fig 6A). Amoebae were co-incubated with live or pre-killed human cells or  
207 incubated in the absence of human cells. Amoebae that had undergone trogocytosis or phagocytosis ingested  
208 a similar amount of human cell material (Fig 6B), however, amoebae were only protected from lysis by human  
209 serum after undergoing trogocytosis (Fig 6C). Therefore, protection from lysis by human serum occurs  
210 specifically after trogocytosis of live cells and not phagocytosis of pre-killed cells.

211 To further distinguish between requirements for trogocytosis and phagocytosis, we next tested  
212 knockdown mutants deficient in rhomboid protease 1 (*EhROM1*) (EHI\_197460), a rhomboid protease with  
213 roles in attachment and ingestion [39,40]. *EhROM1* mutants have been shown to be deficient in both  
214 phagocytosis and pinocytosis, as well as attachment to live cells [39,40]. Furthermore, it has been shown that  
215 silencing of *EhROM1* does not change susceptibility to serum lysis, making these mutants an ideal tool for  
216 testing the effects conferred by ingestion of human cells [39,40]. We generated stable transfectants knocked  
217 down for expression of *EhROM1* (Fig 7A). *EhROM1* knockdown mutants were deficient in attachment to  
218 healthy human cells (Fig 7B-C), consistent with previous studies [40]. Also consistent with previous studies,  
219 *EhROM1* mutant amoebae incubated alone were not more susceptible to serum lysis than control amoebae  
220 (S5B Fig). Using imaging flow cytometry, we assayed *EhROM1* mutants for a trogocytosis defect for the first  
221 time and found that they did not exhibit a defect in trogocytosis of live human cells (Fig 7D, S6 Fig). Consistent  
222 with previous studies [40], we found that *EhROM1* mutants were defective in phagocytosis of pre-killed  
223 human cells (Fig 7E). After co-incubation with live human cells, *EhROM1* mutants were no more or less  
224 protected from lysis by human serum than control amoebae (Fig 7F, S5 Fig). Therefore, a mutant deficient in

225 phagocytosis does not exhibit a difference in protection from serum, further supporting that phagocytosis is  
226 not involved in resistance to lysis by human serum. Moreover, resistance to lysis by human serum is not  
227 associated with simple attachment to human cells, since *EhROM1* mutants are impaired in binding to live  
228 human cells but still exhibit no difference in resistance to human serum. Together, these finding further  
229 underscore that protection from lysis by human serum is associated with trogocytosis, not phagocytosis.

230 Collectively, these results support a new model of immune evasion in which amoebae perform  
231 trogocytosis on live human cells and through trogocytosis, acquire and display human cell membrane proteins.  
232 Display of human cell membrane proteins then leads to protection from human serum, most likely by  
233 inhibiting complement-mediated lysis (Fig 8).

## 234 Discussion

235 In this study, confocal microscopy and imaging flow cytometry experiments revealed that amoebae  
236 acquire and display human cell membrane proteins. This process is actin-dependent and is associated with  
237 resistance to lysis by human serum. Protection from lysis by human serum requires direct contact between  
238 amoebae and human cells, is actin-dependent, and is specifically associated with trogocytosis, not  
239 phagocytosis. Collectively, these data suggest that amoebae acquire and display human cell membrane  
240 proteins through trogocytosis, and that this leads to protection from lysis by human serum complement.

241 Complement resistance by amoebae appears to be relevant to invasive disease. Once amoebae have  
242 invaded intestinal tissue, they can spread from the intestine to the liver through the portal vein [41], and they  
243 can ingest erythrocytes [42], thus they are capable of surviving in the bloodstream. A study that depleted  
244 complement by using cobra venom factor in the hamster model of amoebic liver abscess, found that loss of  
245 complement was correlated with greater severity of liver lesions [43]. Additionally, it was found that serum  
246 from women was more effective in killing amoebae than serum from men, and men are known to be more  
247 susceptible to invasive amoebiasis [44]. Furthermore, pathogenic amoebae have been shown to resist  
248 complement. *E. histolytica* appears to evade complement deposition, while the closely related nonpathogenic  
249 species *Entamoeba dispar* does not [45]. Similarly, amoebae isolated from patients with invasive infection  
250 resist complement, while strains isolated from asymptomatic patients are complement-sensitive [46].

251 Previous studies have hinted that amoebae become more resistant to complement after interacting  
252 with host cells or tissues, and that complement resistance involves proteins on the amoeba surface.  
253 Consistent with our findings, it has previously been demonstrated that amoebae that were made resistant to  
254 complement lysis by hamster liver passage, lost resistance after treatment with trypsin [38], suggesting that  
255 complement-resistance is associated with proteins on the amoeba surface. It has also been shown that  
256 amoebae acquire serum resistance after ingestion of live human erythrocytes, and that resistant amoebae

257 stained positive with antiserum directed to erythrocyte membrane antigens [36]. Though this previous study  
258 described ingestion of erythrocytes as erythrophagocytosis, we now know that amoebae are also capable of  
259 performing trophocytosis on live erythrocytes [19]. In older literature, amoebae were also seen to ingest bites  
260 of erythrocytes in a process that was termed microphagocytosis [47]. Therefore, we propose a model in which  
261 invasive amoebae are able to evade complement detection in the blood by trophocytosis of human cells and  
262 display of human cell membrane proteins.

263 Other mechanisms of complement resistance in *E. histolytica* have been described such as mimicry of  
264 the complement regulatory protein CD59 [48,49], an inhibitor of the membrane attack complex (MAC).  
265 Amoebic cysteine proteinases play a role in cleavage of complement components [50–52]. It has also been  
266 reported that amoebae are made temporarily resistant to complement lysis through treatment with  
267 increasing doses of heat-inactivated human serum, though the mechanism remains unclear [37,53], and it was  
268 recently found that amoebae do not develop resistance to serum from rats by this method [54]. As the  
269 percentage of amoebae lysed after exposure to human serum in our assays never reached 100%, even in  
270 conditions where amoebae were incubated alone, it is likely that multiple factors contribute to complement  
271 resistance in *E. histolytica*. We propose that acquisition of human cell membrane proteins is one of the  
272 mechanisms by which amoebae evade lysis by complement.

273 It will be of great interest to determine which proteins are transferred and displayed on the amoeba  
274 surface. It is possible that complement regulatory proteins such as CD55 or CD46 are displayed by amoebae  
275 and that this directly promotes resistance to complement lysis. Displayed human cell membrane proteins may  
276 also bind to soluble factors in human serum, such as factor H. It is notable that acquired human cell  
277 membrane proteins do not have an even distribution on the amoeba surface, and instead appear in patches.  
278 This was similar for both biotin-streptavidin and MHC-I staining. In mammalian immune cells, similar patchy  
279 localization of acquired membrane proteins has been seen, and this was seen with biotin-streptavidin staining,  
280 fluorescently-tagged proteins, and immunofluorescence [24,28]. It is not clear if the acquired membrane

281 proteins are present in lipid microdomains (*e.g.*, lipid rafts), or are in clusters. It is also possible that while  
282 patchy foci of acquired membrane proteins are clearly seen, these proteins may also be found throughout the  
283 membrane at lower concentrations below the limit of detection. In any case, the distribution of human cell  
284 proteins appears sufficient to confer protection from complement.

285 With the discoveries of amoebic trogocytosis and display of human cell membrane proteins, a new  
286 paradigm for amoeba-human cell interactions is emerging. We previously showed that when amoebae kill  
287 cells, they do not ingest dead cell corpses [19]. Prior to this, amoebae were thought to fully ingest the corpses  
288 of the cells they had killed [5,55,56]. Now, with the discovery of acquisition and display of human cell  
289 membrane proteins, together with the lack of ingestion of cell corpses, a different paradigm is emerging. It is  
290 possible that rather than acquiring nutrition by killing and ingesting entire cells, amoebae nibble and acquire  
291 membrane proteins that contribute to immune evasion. Invasive disease involves survival of amoebae in blood  
292 vessels. Since trogocytosis contributes to tissue invasion [19], it is possible that amoebae acquire human cell  
293 membrane proteins as they invade the intestine. Amoebae would then be equipped to survive in the  
294 bloodstream and to spread to other tissues. Moreover, since there is the potential for a variety of human cell  
295 proteins to be displayed, display of human cell proteins may impact host-amoeba interactions in many ways.

296 Display of human cell proteins acquired during trogocytosis is a novel strategy for immune evasion by a  
297 pathogen. Since other microbial eukaryotes use trogocytosis for cell killing, including *N. fowleri*, there is the  
298 potential for display of acquired membrane proteins to apply to the pathogenesis of other infections.  
299 Furthermore, our studies extend acquisition and display of membrane proteins beyond mammalian immune  
300 cells, suggesting that this may be a fundamental feature of eukaryotic trogocytosis. How membrane proteins  
301 are acquired and displayed by immune cells during trogocytosis is not well understood in immune cells and, to  
302 our knowledge, the underlying mechanism is not under investigation. Thus, ongoing studies in amoebae may  
303 shed light on acquisition and display of membrane proteins during trogocytosis.

304           In summary, we have shown that amoebae display human cell membrane proteins on their surface and  
305 are protected from lysis by human serum after trogocytosis of live human cells. We propose a new model of  
306 immune evasion by *E. histolytica*, whereby amoebae survive complement attack in the blood through  
307 trogocytosis of human cells and display of human cell membrane proteins. This work broadens our  
308 understanding of trogocytosis as a conserved feature of eukaryotic biology, as well as our understanding of  
309 the pathogenesis of amoebiasis.

## 310 **Materials and Methods**

### 311 **Cell culture**

312 HM1: IMSS (ATCC) *E. histolytica* trophozoites (amoebae) were cultured at 35°C in Trypticase-Yeast  
313 Extract-Iron-Serum (TYI-S-33) media supplemented with 80 Units/mL penicillin and 80 µg/mL streptomycin  
314 (Gibco), 2.3% Diamond Vitamin Tween 80 Solution 40x (Sigma-Aldrich) and 15% heat-inactivated adult bovine  
315 serum (Gemini Bio-Products). Amoebae were harvested when tissue culture flasks reached 80-100%  
316 confluency and then resuspended in M199s media (Gibco medium M199 with Earle's Salts, L-Glutamine, 2.2  
317 g/L Sodium Bicarbonate and without Phenol Red) supplemented with 5.7 mM L-cysteine (Sigma-Aldrich), 25  
318 mM HEPES (Sigma-Aldrich) and 0.5% bovine serum albumin (Gemini Bio-Products).

319 Human Jurkat T cells from ATCC (Clone E6-1) were cultured at 37°C and 5% CO<sub>2</sub> in RPMI Medium 1640  
320 (Gibco RPMI with L-Glutamine and without Phenol Red) supplemented with 10 mM HEPES (Affymetrix), 100  
321 Units/mL penicillin and 100 µg/mL streptomycin (Gibco) and 10% heat-inactivated fetal bovine serum (Gibco).  
322 human cells were harvested between 5x10<sup>5</sup> and 2x10<sup>6</sup> cells/ml and resuspended in M199s media.

### 323 **Generation of *EhROM1* mutants**

324 The *EhROM1* silencing construct, made from a pEhEx plasmid backbone, was generated by Morf *et al.*  
325 as described in [57]. The construct contained 132 base pairs of the trigger gene EHI\_048600 fused to the first  
326 537 base pairs of *EhROM1* (EHI\_197460). Amoebae were transfected with 20 µg of the *EhROM1* silencing  
327 construct using Attractene Transfection Reagent (QIAGEN). Transfectants were then maintained under  
328 selection with Geneticin at 6 µg/ml. Clonal lines were generated by limiting dilution in a 96-well plate  
329 contained in a BD GasPak EZ Pouch System (BD Biosciences), and silencing was confirmed with RT-PCR. An  
330 individual clonal line was used for all experiments. A vector control line was generated by transfection with  
331 the pEhEx-trigger construct backbone, using the same approach.

### 332 Confocal immunofluorescence assays

333 Amoebae were washed and labeled in M199s with CellTracker Green CMFDA Dye (Invitrogen) at 310  
334 ng/ml for 10 minutes at 35°C. In the biotin transfer experiments, human cells were resuspended in 1X  
335 Dulbecco's Phosphate Buffered Saline (PBS: Sigma-Aldrich) and then biotinylated with EZ-Link Sulfo-NHS-SS-  
336 Biotin (Thermo Fisher Scientific) at 480 µg/ml in 1X PBS for 25 minutes at 4°C. 1M Tris-HCL pH 8 was added to  
337 the samples for a final concentration of 100 mM to quench the reaction. Cells were next washed in 1X PBS  
338 containing Tris-HCL pH 8 at 100 mM, and then resuspended in M199s. Amoebae and human cells were  
339 combined at a 1:5 ratio in M199s and co-incubated for 5 minutes at 35°C. Following co-incubation, cells were  
340 fixed with 4% paraformaldehyde (Electron Microscopy Sciences) for 30 minutes at room temperature and  
341 stained with an Alexa Fluor 633 streptavidin conjugate (Invitrogen) at 20 µg/ml for 1 hour at 4°C. After  
342 fixation, samples were stained with DAPI (Sigma-Aldrich) for 10 minutes at room temperature. Samples were  
343 then incubated on coverslips pre-coated with collagen (Collagen I, Rat Tail: Gibco), according to the  
344 manufacturer's instructions, for 1 hour at room temperature and mounted on glass slides using VECTASHIELD  
345 Antifade Mounting Medium (Vector Laboratories). In some experiments, samples were incubated on  
346 Superfrost Plus Micro Slides (VWR) for 1 hour, and coverslips were then mounted with VECTASHIELD Antifade  
347 Mounting Medium. Samples were imaged on an Olympus FV1000 laser point-scanning confocal microscope or  
348 on an Intelligent Imaging Innovations Hybrid Spinning Disk Confocal-TIRF-Widefield Microscope. Images were  
349 collected from 4 independent experiments.

350 For the MHC class I immunofluorescence experiments, human cells were washed and resuspended in  
351 M199s but left unlabeled before co-incubation with amoebae. Amoebae and human cells were combined at a  
352 1:5 ratio in M199s and co-incubated for 5 minutes at 35°C. Following co-incubation and fixation, samples were  
353 blocked for 1 hour in PBS-T (0.1% Tween 20 in 1X PBS) supplemented with 20% Goat Serum (Jackson  
354 Immunoresearch Labs Inc.) and 5% bovine serum albumin (Gemini Bio-Products). Samples were then washed

355 in PBS-T and incubated overnight with an MHC class I monoclonal primary antibody (Thermo Fisher Scientific  
356 HLA-ABC Monoclonal Antibody W6/32) at 10 µg/ul, followed by washing with PBS-T and incubation with an  
357 anti-mouse Cy3 secondary antibody (Jackson ImmunoResearch Labs Inc.) at 3.5 ng/ml at room temperature for  
358 1 hour. Samples were stained with DAPI and mounted on glass slides as above. Images were collected from 4  
359 independent experiments.

### 360 **Imaging flow cytometry immunofluorescence assays**

361 Amoebae were resuspended in M199s media and pretreated with cytochalasin D from *Zygosporium*  
362 *mansonii* (Sigma-Aldrich) at 20 µM or with the equivalent volume of dimethylsulfoxide (DMSO) for 1 hour at  
363 35°C. Cytochalasin D and DMSO were kept in the media for the duration of the experiment. Following pre-  
364 treatment, amoebae were labeled with CellTracker Green CMFDA Dye (Invitrogen) at 93 ng/ml for 10 minutes  
365 at 35°C. Human cells were labeled in culture with Hoechst 33342 (Invitrogen) at 5 µg/ml for 1 hour at 37°C  
366 and then resuspended in 1X PBS. Human cells were then biotinylated with EZ-Link Sulfo-NHS-SS-Biotin  
367 (Thermo Fisher Scientific) at 480 µg/ml in 1X PBS for 25 minutes at 4°C. 100 mM Tris-HCL pH 8 was used to  
368 quench the reaction, cells were washed in 100 mM Tris-HCL pH 8 and were resuspended in M199s. Amoebae  
369 and human cells were combined at a 1:5 ratio in M199s and co-incubated for 5 minutes at 35°C. After co-  
370 incubation, samples were immediately placed on ice to halt ingestion, stained with an Alexa Fluor 633  
371 streptavidin conjugate (Invitrogen) at 20 µg/ml for 1 hour at 4°C and fixed with 4% paraformaldehyde  
372 (Electron Microscopy Sciences) for 30 minutes at room temperature. Fixed samples were resuspended in 1X  
373 PBS and run on an Amnis ImageStreamX Mark II. 10,000 events per sample were collected from 6 repeats  
374 across three independent experiments.

### 375 **Serum lysis assays**

376 Amoebae were washed and labeled in M199s with CellTracker Green CMFDA Dye (Invitrogen) at 93  
377 ng/ml for 10 minutes at 35°C. Human cells were washed and labeled in M199s with Diic18(5)-Ds [1,1-

378 Diocadecyl-3,3,3,3-Tetramethylindodicarbocyanine-5,5-Disulfonic Acid] (DiD: Assay Biotech) at 21  $\mu\text{g}/\text{ml}$  for 5  
379 minutes at 37°C and 10 minutes at 4°C. After washing with M199s, amoebae and human cells were combined  
380 at a 1:5 ratio in M199s and co-incubated for 1 hour at 35°C, or amoebae were incubated in the same  
381 conditions in the absence of human cells. Next, cells were pelleted at 400 x *g* for 8 minutes and were  
382 resuspended in 100% normal human serum (Pooled Normal Human Complement Serum, Innovative Research  
383 Inc.), heat-inactivated human serum (inactivated at 56°C for 30 minutes), or M199s. Serum/media was  
384 supplemented with 150  $\mu\text{M}$   $\text{CaCl}_2$  and 150  $\mu\text{M}$   $\text{MgCl}_2$  (Fig. S2). Next, cells were incubated for 30 minutes at  
385 35°C. Cells were then washed and resuspended in M199s media and incubated with LIVE/DEAD Fixable Violet  
386 Dead Cell Stain (Invitrogen) that was prepared according to the manufacturer's instructions, at 4  $\mu\text{l}/\text{ml}$  for 30  
387 minutes on ice. Next, samples were fixed with 4% paraformaldehyde (Electron Microscopy Sciences) for 30  
388 minutes at room temperature. Fixed samples were pelleted and resuspended in 1X PBS, then run on an Amnis  
389 ImageStreamX Mark II. 10,000 events per sample were collected.

390 In the cytochalasin D experiments, amoebae were pretreated with cytochalasin D from *Zygosporium*  
391 *mansonii* (Sigma-Aldrich) at 20  $\mu\text{M}$  or an equivalent volume of DMSO for 1 hour at 35°C. Cytochalasin D/DMSO  
392 was kept in the media for the duration of the experiment. In experiments where amoebae ingested live or pre-  
393 killed cells, human cells were pretreated in culture with staurosporine from *Streptomyces* sp. (Sigma-Aldrich)  
394 at 1  $\mu\text{M}$  or with the equivalent volume of DMSO overnight at 37°C. Human cells were then washed and  
395 suspended in M199s media and labeled with CellTracker Deep Red (CTDR) (Invitrogen) at 1  $\mu\text{M}$  for 30 minutes  
396 at 37°C. In transwell assays, amoebae and human cells were incubated together at a 1:5 ratio or separately in  
397 12 mm transwells with 3.0  $\mu\text{m}$  pore, 10  $\mu\text{m}$  thick polycarbonate membrane inserts (Corning). In experiments  
398 using EhROM1 knockdown, stably transfected *EhROM1* clonal mutants were compared to mutants that  
399 contained a pEhEx-trigger backbone vector control construct.

#### 400 **Ingestion assays**

401 In trogocytosis assays, CMFDA labeled transfectants were incubated alone or in the presence of live  
402 DiD-labeled Jurkat cells for 0, 5, 20, 40 or 80 minutes. Samples were then labeled with Live/Dead Violet and  
403 fixed with 4% paraformaldehyde. Internalization of human cell material was quantified using imaging flow  
404 cytometry. In phagocytosis assays, human cells were heat-killed at 60°C for 40 minutes and were labeled with  
405 CTDR and Hoechst prior to incubation with CMFDA labeled amoebae.

#### 406 **Attachment assay**

407 CMFDA labeled amoebae were combined with CTDR labeled live human cells at a 1:5 ratio, centrifuged  
408 at 150 x g for 5 minutes 4°C, and incubated on ice for 1 hour. Samples were then fixed with 4%  
409 paraformaldehyde. Samples were incubated on Superfrost Plus Micro Slides (VWR) for 1 hour, coverslips were  
410 mounted with VECTASHIELD Antifade Mounting Medium and slides were imaged on an Intelligent Imaging  
411 Innovations Hybrid Spinning Disk Confocal-TIRF-Widefield Microscope. 20 images were collected per slide.  
412 Amoebae with 3 or more attached human cells were scored as attachment positive. Image collection and  
413 scoring were performed in a blinded manner.

#### 414 **Imaging flow cytometry analysis**

415 Samples were run on an Amnis ImageStreamX Mark II and 10,000 events were collected per sample.  
416 Data were analyzed using Amnis IDEAS software. Samples were gated on focused cells, single amoebae,  
417 amoebae that had come in contact with human cells, and amoebae that had internalized human material.  
418 From the single amoebae gate, amoebic death was quantified by plotting intensity of LIVE/DEAD Violet against  
419 side scatter and gating on LIVE/DEAD Violet positive cells (see Fig. S3).

420 In the biotin transfer experiment, single amoebae were divided into Hoechst high and Hoechst low  
421 populations in order to isolate single amoebae with and without human cells. Overlap of biotin with CMFDA  
422 labeled amoebae was plotted and biotin positive cells were selected from both Hoechst high and low  
423 populations (see Fig. S1).

424 In the trogocytosis and phagocytosis assays, focused cells were gated from total collected events. Next,  
425 single cells were gated, and then single amoebae were gated. Amoebae positive for human cells were gated  
426 and internalization of human cells was measured. (see Fig. S5)

#### 427 **Statistical analysis**

428 All statistical analysis was performed using GraphPad Prism. All data plots display means and standard  
429 deviation values. Data were statistically analyzed using a student's unpaired t-test (ns =  $P > 0.05$ , \* =  $P \leq 0.05$ ,  
430 \*\* =  $P \leq 0.01$ , \*\*\* =  $P \leq 0.001$ , \*\*\*\* =  $P \leq 0.0001$ ).

## 431 **Acknowledgements**

432 We thank the MCB Light Microscopy Imaging Facility at UC Davis for technical assistance. We thank Dr.

433 Stephen McSorley and the members of our laboratory for helpful discussions.

## 434 References

- 435 1. Haque R, Mondal D, Kirkpatrick BD, Akther S, Farr BM, Sack RB, et al. Epidemiologic and clinical  
436 characteristics of acute diarrhea with emphasis on *Entamoeba histolytica* infections in preschool children  
437 in an urban slum of Dhaka, Bangladesh. *Am J Trop Med Hyg.* 2003;69: 398–405.
- 438 2. Speich B, Croll D, Fürst T, Utzinger J, Keiser J. Effect of sanitation and water treatment on intestinal  
439 protozoa infection: a systematic review and meta-analysis. *The Lancet Infectious Diseases.* 2016;16: 87–  
440 99. doi:10.1016/S1473-3099(15)00349-7
- 441 3. Petri WA, Mondal D, Peterson KM, Duggal P, Haque R. Association of malnutrition with amebiasis. *Nutr*  
442 *Rev.* 2009;67: S207–S215. doi:10.1111/j.1753-4887.2009.00242.x
- 443 4. Gilchrist CA, Petri SE, Schneider BN, Reichman DJ, Jiang N, Begum S, et al. Role of the Gut Microbiota of  
444 Children in Diarrhea Due to the Protozoan Parasite *Entamoeba histolytica*. *J Infect Dis.* 2016;213: 1579–  
445 1585. doi:10.1093/infdis/jiv772
- 446 5. Ralston KS, Petri WA. Tissue destruction and invasion by *Entamoeba histolytica*. *Trends Parasitol.* 2011;27:  
447 254–263. doi:10.1016/j.pt.2011.02.006
- 448 6. Ravdin JI, Croft BY, Guerrant RL. Cytopathogenic mechanisms of *Entamoeba histolytica*. *J Exp Med.*  
449 1980;152: 377–390.
- 450 7. Ravdin JI, Guerrant RL. Studies on the cytopathogenicity of *Entamoeba histolytica*. *Arch Invest Med (Mex).*  
451 1980;11: 123–128.
- 452 8. Ravdin JI, Guerrant RL. Role of Adherence in Cytopathogenic Mechanisms of *Entamoeba Histolytica*. *J Clin*  
453 *Invest.* 1981;68: 1305–1313.
- 454 9. Saffer LD, Petri WA. Role of the galactose lectin of *Entamoeba histolytica* in adherence-dependent killing  
455 of mammalian cells. *Infect Immun.* 1991;59: 4681–4683.
- 456 10. Thibeaux R, Dufour A, Roux P, Bernier M, Baglin A-C, Frileux P, et al. Newly visualized fibrillar collagen  
457 scaffolds dictate *Entamoeba histolytica* invasion route in the human colon. *Cell Microbiol.* 2012;14: 609–  
458 621. doi:10.1111/j.1462-5822.2012.01752.x
- 459 11. Hellberg A, Nickel R, Lotter H, Tannich E, Bruchhaus I. Overexpression of cysteine proteinase 2 in  
460 *Entamoeba histolytica* or *Entamoeba dispar* increases amoeba-induced monolayer destruction in vitro  
461 but does not augment amoebic liver abscess formation in gerbils. *Cell Microbiol.* 2001;3: 13–20.
- 462 12. Keene WE, Petitt MG, Allen S, McKerrow JH. The major neutral proteinase of *Entamoeba histolytica*. *J Exp*  
463 *Med.* 1986;163: 536–549.
- 464 13. Lidell ME, Moncada DM, Chadee K, Hansson GC. *Entamoeba histolytica* cysteine proteases cleave the  
465 MUC2 mucin in its C-terminal domain and dissolve the protective colonic mucus gel. *Proc Natl Acad Sci*  
466 *USA.* 2006;103: 9298–9303. doi:10.1073/pnas.0600623103
- 467 14. Bracha R, Nuchamowitz Y, Leippe M, Mirelman D. Antisense inhibition of amoebapore expression in  
468 *Entamoeba histolytica* causes a decrease in amoebic virulence. *Mol Microbiol.* 1999;34: 463–472.

- 469 15. Bracha R, Nuchamowitz Y, Mirelman D. Transcriptional silencing of an amoebapore gene in *Entamoeba*  
470 *histolytica*: molecular analysis and effect on pathogenicity. *Eukaryotic Cell*. 2003;2: 295–305.
- 471 16. Leippe M, Andrä J, Müller-Eberhard HJ. Cytolytic and antibacterial activity of synthetic peptides derived  
472 from amoebapore, the pore-forming peptide of *Entamoeba histolytica*. *Proc Natl Acad Sci USA*. 1994;91:  
473 2602–2606.
- 474 17. Leippe M, Andrä J, Nickel R, Tannich E, Müller-Eberhard HJ. Amoebapores, a family of membranolytic  
475 peptides from cytoplasmic granules of *Entamoeba histolytica*: isolation, primary structure, and pore  
476 formation in bacterial cytoplasmic membranes. *Mol Microbiol*. 1994;14: 895–904.
- 477 18. Ravdin JI, Moreau F, Sullivan JA, Petri WA, Mandell GL. Relationship of free intracellular calcium to the  
478 cytolytic activity of *Entamoeba histolytica*. *Infect Immun*. 1988;56: 1505–1512.
- 479 19. Ralston KS, Solga MD, Mackey-Lawrence NM, Somlata, Bhattacharya A, Petri Jr WA. Trophocytosis by  
480 *Entamoeba histolytica* contributes to cell killing and tissue invasion. *Nature*. 2014;508: 526–530.  
481 doi:10.1038/nature13242
- 482 20. Ralston KS. Taking a bite: Amoebic trophocytosis in *Entamoeba histolytica* and beyond. *Current Opinion in*  
483 *Microbiology*. 2015;28: 26–35. doi:10.1016/j.mib.2015.07.009
- 484 21. Brown T. Observations by immunofluorescence microscopy and electron microscopy on the  
485 cytopathogenicity of *naegleria fowleri* in mouse embryo-cell cultures. *Journal of Medical Microbiology*.  
486 1979;12: 363–371. doi:10.1099/00222615-12-3-363
- 487 22. Waddell DR, Vogel G. Phagocytic behavior of the predatory slime mold, *Dictyostelium caveatum*. *Cell*  
488 *Nibbling*. *Exp Cell Res*. 1985;159: 323–334.
- 489 23. Batista FD, Iber D, Neuberger MS. B cells acquire antigen from target cells after synapse formation. *Nature*.  
490 2001;411: 489–494. doi:10.1038/35078099
- 491 24. Wakim LM, Bevan MJ. Cross-dressed dendritic cells drive memory CD8+ T-cell activation after viral  
492 infection. *Nature*. 2011;471: 629–632. doi:10.1038/nature09863
- 493 25. Davis CO, Kim K-Y, Bushong EA, Mills EA, Boassa D, Shih T, et al. Transcellular degradation of axonal  
494 mitochondria. *Proc Natl Acad Sci USA*. 2014;111: 9633–9638. doi:10.1073/pnas.1404651111
- 495 26. Weinhard L, di Bartolomei G, Bolasco G, Machado P, Schieber NL, Neniskyte U, et al. Microglia remodel  
496 synapses by presynaptic trophocytosis and spine head filopodia induction. *Nat Commun*. 2018;9: 1228.  
497 doi:10.1038/s41467-018-03566-5
- 498 27. Abdu Y, Maniscalco C, Heddleston JM, Chew T-L, Nance J. Developmentally programmed germ cell  
499 remodelling by endodermal cell cannibalism. *Nat Cell Biol*. 2016;18: 1302–1310. doi:10.1038/ncb3439
- 500 28. Steele S, Radlinski L, Taft-Benz S, Brunton J, Kawula TH. Trophocytosis-associated cell to cell spread of  
501 intracellular bacterial pathogens. Monack D, editor. *eLife*. 2016;5: e10625. doi:10.7554/eLife.10625
- 502 29. Mercer F, Ng SH, Brown TM, Boatman G, Johnson PJ. Neutrophils kill the parasite *Trichomonas vaginalis*  
503 using trophocytosis. *PLoS Biol*. 2018;16: e2003885. doi:10.1371/journal.pbio.2003885

- 504 30. Matlung HL, Babes L, Zhao XW, van Houdt M, Treffers LW, van Rees DJ, et al. Neutrophils Kill Antibody-  
505 Oponized Cancer Cells by Trogoptosis. *Cell Rep.* 2018;23: 3946-3959.e6.  
506 doi:10.1016/j.celrep.2018.05.082
- 507 31. Velmurugan R, Challa DK, Ram S, Ober RJ, Ward ES. Macrophage-Mediated Trogocytosis Leads to Death of  
508 Antibody-Oponized Tumor Cells. *Mol Cancer Ther.* 2016;15: 1879–1889. doi:10.1158/1535-7163.MCT-  
509 15-0335
- 510 32. Miyake K, Shiozawa N, Nagao T, Yoshikawa S, Yamanishi Y, Karasuyama H. Trogocytosis of peptide-MHC  
511 class II complexes from dendritic cells confers antigen-presenting ability on basophils. *Proc Natl Acad Sci*  
512 *USA.* 2017;114: 1111–1116. doi:10.1073/pnas.1615973114
- 513 33. Gu P, Gao JF, D’Souza CA, Kowalczyk A, Chou K-Y, Zhang L. Trogocytosis of CD80 and CD86 by induced  
514 regulatory T cells. *Cell Mol Immunol.* 2012;9: 136–146. doi:10.1038/cmi.2011.62
- 515 34. Rossi EA, Goldenberg DM, Michel R, Rossi DL, Wallace DJ, Chang C-H. Trogocytosis of multiple B-cell  
516 surface markers by CD22 targeting with epratuzumab. *Blood.* 2013;122: 3020–3029. doi:10.1182/blood-  
517 2012-12-473744
- 518 35. Martínez-Martín N, Fernández-Arenas E, Cemerski S, Delgado P, Turner M, Heuser J, et al. T cell receptor  
519 internalization from the immunological synapse is mediated by TC21 and RhoG GTPase-dependent  
520 phagocytosis. *Immunity.* 2011;35: 208–222. doi:10.1016/j.immuni.2011.06.003
- 521 36. Gutiérrez-Kobeh L, Cabrera N, Pérez-Montfort R. A Mechanism of Acquired Resistance to Complement-  
522 Mediated Lysis by *Entamoeba histolytica*. *The Journal of Parasitology.* 1997;83: 234–241.  
523 doi:10.2307/3284446
- 524 37. Hamelmann C, Foerster B, Burchard GD, Shetty N, Horstmann RD. Induction of complement resistance in  
525 cloned pathogenic *Entamoeba histolytica*. *Parasite Immunol.* 1993;15: 223–228.
- 526 38. Hamelmann C, Urban B, Foerster B, Horstmann RD. Complement resistance of pathogenic *Entamoeba*  
527 *histolytica* mediated by trypsin-sensitive surface component(s). *Infect Immun.* 1993;61: 1636–1640.
- 528 39. Rastew E, Morf L, Singh U. *Entamoeba histolytica* rhomboid protease 1 has a role in migration and motility  
529 as validated by two independent genetic approaches. *Exp Parasitol.* 2015;154: 33–42.  
530 doi:10.1016/j.exppara.2015.04.004
- 531 40. Baxt LA, Rastew E, Bracha R, Mirelman D, Singh U. Downregulation of an *Entamoeba histolytica* Rhomboid  
532 Protease Reveals Roles in Regulating Parasite Adhesion and Phagocytosis. *Eukaryot Cell.* 2010;9: 1283–  
533 1293. doi:10.1128/EC.00015-10
- 534 41. Rigother M-C, Khun H, Tavares P, Cardona A, Huerre M, Guillén N. Fate of *Entamoeba histolytica* during  
535 establishment of amoebic liver abscess analyzed by quantitative radioimaging and histology. *Infect*  
536 *Immun.* 2002;70: 3208–3215.
- 537 42. González-Ruiz A, Haque R, Aguirre A, Castañón G, Hall A, Guhl F, et al. Value of microscopy in the diagnosis  
538 of dysentery associated with invasive *Entamoeba histolytica*. *J Clin Pathol.* 1994;47: 236–239.
- 539 43. Capin R, Capin NR, Carmona M, Ortiz-Ortiz L. Effect of complement depletion on the induction of amebic  
540 liver abscess in the hamster. *Arch Invest Med (Mex).* 1980;11: 173–180.

- 541 44. Snow M, Chen M, Guo J, Atkinson J, Stanley SL. Differences in complement-mediated killing of *Entamoeba*  
542 *histolytica* between men and women--an explanation for the increased susceptibility of men to invasive  
543 amebiasis? *Am J Trop Med Hyg.* 2008;78: 922–923.
- 544 45. Costa CA, Nunes AC, Ferreira AJ, Gomes MA, Caliri MV. *Entamoeba histolytica* and *E. dispar* trophozoites  
545 in the liver of hamsters: in vivo binding of antibodies and complement. *Parasit Vectors.* 2010;3: 23.  
546 doi:10.1186/1756-3305-3-23
- 547 46. Reed SL, Curd JG, Gigli I, Gillin FD, Braude AI. Activation of complement by pathogenic and nonpathogenic  
548 *Entamoeba histolytica*. *J Immunol.* 1986;136: 2265–2270.
- 549 47. Lejeune A, Gicquaud C. Evidence for two mechanisms of human erythrocyte endocytosis by *Entamoeba*  
550 *histolytica*-like amoebae (Laredo strain). *Biol Cell.* 1987;59: 239–245.
- 551 48. Braga LL, Ninomiya H, McCoy JJ, Eacker S, Wiedmer T, Pham C, et al. Inhibition of the complement  
552 membrane attack complex by the galactose-specific adhesion of *Entamoeba histolytica*. *J Clin Invest.*  
553 1992;90: 1131–1137. doi:10.1172/JCI115931
- 554 49. Ventura-Juárez J, Campos-Rodríguez R, Jarillo-Luna RA, Muñoz-Fernández L, Escario-G-Trevijano JA, Pérez-  
555 Serrano J, et al. Trophozoites of *Entamoeba histolytica* express a CD59-like molecule in human colon.  
556 *Parasitol Res.* 2009;104: 821–826. doi:10.1007/s00436-008-1262-3
- 557 50. Reed SL, Ember JA, Herdman DS, DiScipio RG, Hugli TE, Gigli I. The extracellular neutral cysteine proteinase  
558 of *Entamoeba histolytica* degrades anaphylatoxins C3a and C5a. *J Immunol.* 1995;155: 266–274.
- 559 51. Reed SL, Gigli I. Lysis of complement-sensitive *Entamoeba histolytica* by activated terminal complement  
560 components. Initiation of complement activation by an extracellular neutral cysteine proteinase. *J Clin*  
561 *Invest.* 1990;86: 1815–1822. doi:10.1172/JCI114911
- 562 52. Reed SL, Keene WE, McKerrow JH, Gigli I. Cleavage of C3 by a neutral cysteine proteinase of *Entamoeba*  
563 *histolytica*. *J Immunol.* 1989;143: 189–195.
- 564 53. Calderon J, Tovar R. Loss of susceptibility to complement lysis in *Entamoeba histolytica* HM1 by treatment  
565 with human serum. *Immunology.* 1986;58: 467–471.
- 566 54. Olivos-García A, Nequiz M, Liceaga S, Mendoza E, Zúñiga P, Cortes A, et al. Complement is a rat natural  
567 resistance factor to amoebic liver infection. *Biosci Rep.* 2018;38. doi:10.1042/BSR20180713
- 568 55. Huston CD, Boettner DR, Miller-Sims V, Petri, Jr. WA. Apoptotic Killing and Phagocytosis of Host Cells by  
569 the Parasite *Entamoeba histolytica*. *Infect Immun.* 2003;71: 964–972. doi:10.1128/IAI.71.2.964-972.2003
- 570 56. Sateriale A, Huston CD. A Sequential Model of Host Cell Killing and Phagocytosis by *Entamoeba histolytica*.  
571 *J Parasitol Res.* 2011;2011. doi:10.1155/2011/926706
- 572 57. Khalil MI, Foda BM, Suresh S, Singh U. Technical advances in trigger-induced RNA interference gene  
573 silencing in the parasite *Entamoeba histolytica*. *Int J Parasitol.* 2016;46: 205–212.  
574 doi:10.1016/j.ijpara.2015.11.004



## 577 **Figure Captions**

### 578 **Fig 1. Following interaction with human cells, human cell membrane proteins are displayed by amoebae**

579 **(A)** Human cell membrane proteins were labeled with biotin prior to co-incubation with CMFDA-labeled  
580 amoebae. Cells were co-incubated for 5 minutes and immediately fixed. Following fixation, samples were  
581 labeled with fluorescently-conjugated streptavidin and DAPI. **(B)** Representative images of amoebae incubated  
582 alone or co-incubated with biotinylated human cells. Amoebae are shown in green and streptavidin is shown  
583 in red. Nuclei are shown in blue. Arrow indicates a patch of biotin-streptavidin localized to the amoeba  
584 surface. **(C)** 3D rendering of Z stack images taken from panel B. Arrow indicates transferred biotin. **(D)** Human  
585 cells were labeled with cell tracker deep red (CTDR) prior to co-incubation with CMFDA-labeled amoebae. Cells  
586 were co-incubated for 5 minutes and immediately fixed. Following fixation, samples were labeled with DAPI  
587 and MHC-I was detected using immunofluorescence. **(E)** Representative images of amoebae incubated alone  
588 or co-incubated with CTDR-labeled human cells. Amoebae are shown in green, human cell cytoplasm is shown  
589 in red, MHC-I is shown in yellow and nuclei are shown in blue. Arrow indicates MHC-I present on the amoeba  
590 surface. **(F)** 3D rendering of Z stack images taken from E. Arrow indicates transferred MHC-I. For panels B-F,  
591 images were collected from 4 independent experiments.

### 592 **Fig 2. Acquisition of human cell membrane proteins is inhibited with cytochalasin D treatment**

593 CMFDA-labeled amoebae were pre-treated with either cytochalasin D (Cyto. D) or DMSO (Control) and were  
594 then combined with Hoechst-labeled human cells. Immediately after co-incubation, cells were placed on ice  
595 to halt ingestion and stained with fluorescently-conjugated streptavidin. Samples were quantitatively analyzed  
596 using imaging flow cytometry, with 10,000 images collected for each sample. **(A)** Gate used to identify single  
597 amoebae from total cells. Focused cells were gated on single amoebae using aspect ratio and intensity of  
598 CMFDA fluorescence. **(B)** Representative plots of images with and without human cell nuclei (Hoechst high or  
599 low populations) are shown. The Hoechst high population contained images of amoebae with human cells and

600 the Hoechst low population contained images of amoebae without human cells. **(C)** Overlap of biotin and  
601 CMFDA fluorescence was measured, and biotin positive images were gated. Representative plots of DMSO and  
602 cytochalasin D treated samples are shown. **(D)** Quantification of plots from panel B. DMSO treated samples  
603 are shown in blue and cytochalasin D treated samples are shown in orange. **(E)** Quantification of plots from  
604 panel C. **(F)** Representative images of the populations shown in panel C. Amoebae are shown in green, cell  
605 nuclei are shown in blue, and biotin is shown in magenta. Arrows indicate patches of transferred biotin. Whole  
606 human cells with stained nuclei are marked with asterisks. n=6 from 3 independent experiments.

### 607 **Fig 3. Interaction with human cells leads to protection from lysis by human serum**

608 **(A)** CMFDA-labeled amoebae were incubated alone or in the presence of DiD-labeled human cells for 1 hour.  
609 Cells were then exposed to either active human serum, heat-inactivated human serum, or M199s medium.  
610 Following exposure to serum, samples were stained with Live/Dead Violet and viability was quantified using  
611 imaging flow cytometry, with 10,000 images collected for each sample. **(B)** Representative plots showing  
612 internalization of human cells in each condition. **(C)** Representative plots comparing amoebic death in the  
613 active serum, and heat-inactivated serum conditions. **(D)** Quantification of amoebic death for all experimental  
614 conditions. Cells exposed to M199s medium are shown in grey, heat-inactivated human serum in red, and  
615 active human serum in blue. % Death was normalized to the amoeba alone samples that were treated with  
616 active human serum. **(E)** Representative images of live and dead amoebae from amoebae co-incubated with  
617 human cells and exposed to active human serum. Amoebae are shown in green, human cells in red, and dead  
618 cells in violet. n=10 from 5 independent experiments.

### 619 **Fig 4. Protection from human serum lysis is dependent on contact with human cells**

620 **(A)** Depiction of each transwell condition used in panels B-C. CMFDA-labeled amoebae and DiD-labeled human  
621 cells were incubated alone, together or separately in four different transwell conditions. Condition 1:  
622 amoebae alone in the lower chamber; condition 2: amoebae and human cells together in the lower chamber;

623 condition 3: human cells in the upper chamber and amoebae in the lower chamber; and condition 4: amoebae  
624 and human cells together in the upper chamber and amoebae in the lower chamber. Cells were co-incubated  
625 in transwells for 1 hour and then cells from the lower chambers were harvested, exposed to human serum and  
626 analyzed. Viability was assessed using Live/Dead Violet dye and imaging flow cytometry **(B)** Quantification of  
627 human cell positive amoebae in conditions 1-4. **(C)** Quantification of amoebic death in conditions 1-4 from  
628 panel A. % Death was normalized to amoebae alone (condition 1). n=10 from 5 independent experiments.

629 **Fig 5. Protection from human serum is actin-dependent.**

630 CMFDA labeled amoebae were incubated alone or in the presence of DiD-labeled human cells for 1 hour and  
631 then exposed to active human serum. Samples were then stained with Live/Dead Violet viability dye and  
632 analyzed by imaging flow cytometry. **(A)** Amoebae were either pretreated with cytochalasin D (light grey) or  
633 DMSO (dark grey) for 1 hour. Quantification of internalization of human cells. **(B)** Quantification of amoebic  
634 death is shown. % Death has been normalized to the amoeba alone DMSO-treated samples. n=6 from 3  
635 independent experiments.

636 **Fig 6. Protection requires trogocytosis but not phagocytosis of human cells.**

637 **(A)** Human cells were pretreated with staurosporine (dark grey) or DMSO (light grey). The human cell viability  
638 before co-incubation is shown. **(B)** Quantification of human cell internalization by amoebae. **(C)** Quantification  
639 of amoebic death. % Death was normalized to the amoebae alone samples. n=8 from 4 independent  
640 experiments.

641 **Fig 7. *EhROM1* knockdown mutants defective in phagocytosis but not trogocytosis are protected from**  
642 **serum lysis.**

643 Amoebae were stably transfected with an *EhROM1* knockdown plasmid (*EhROM1*) or vector control plasmid  
644 (Control). **(A)** Silencing of *EhROM1* was verified by using RT-PCR. Reverse transcriptase (RT) was included (+),

645 or omitted (-) as a control. GAPDH was used to control for loading. **(B)** *EhROM1* and vector control  
646 transfectants were incubated on ice with live human cells for 1 hour, then fixed and analyzed using confocal  
647 microscopy. The percentage of amoebae with 3 or more attached human cells for each condition is displayed;  
648 vector control is shown with open bars and the *EhROM1* knockdown mutant is shown with blue bars. n=4  
649 replicates from 2 independent experiments. 20 images were collected per slide and 195-252 individual  
650 amoebae were counted per condition. **(C)** Representative images from panel B. Amoebae are shown in green  
651 and human cells are shown in red. Arrow indicates an amoeba with a rosette of attached human cells. **(D)**  
652 CMFDA-labeled *EhROM1* knockdown mutants (blue circles) or vector control (open circles) transfectants were  
653 incubated alone or in the presence of live DiD-labeled human cells for 0, 5, 20, 40 or 80 minutes.  
654 Internalization of human cell material was quantified using imaging flow cytometry. n=20 from 10  
655 independent experiments. **(E)** CMFDA-labeled *EhROM1* knockdown mutants (blue circles) or vector control  
656 (open circles) transfectants were incubated alone or in the presence of heat-killed CTDR-labeled human cells  
657 for 0, 5, 20, 40 or 80 minutes. Internalization of human cell material was quantified using imaging flow  
658 cytometry. n=4 from 2 independent experiments. **(F)** *EhROM1* (blue bar) or vector control (open bar) amoebae  
659 were co-incubated with live human cells for 1 hour, and then exposed to human serum. Viability was assessed  
660 using Live/Dead Violet dye and imaging flow cytometry. % protection was calculated by subtracting the total  
661 lysis of amoebae co-incubated with human cells from the total lysis of amoebae incubated alone. n= 9-10 from  
662 5 independent experiments. Protection data displays means of 2 replicates from all 5 experiments.

663 **Fig 8. Proposed model of protection from serum lysis.**

664 Amoebae encounter live human cells while invading the intestine or disseminating in the blood stream and  
665 perform trogocytosis. Trogocytosis leads to acquisition and display of human cell membrane proteins on the  
666 amoebae surface. Display of human cell proteins then protects the amoebae from lysis in the blood by  
667 inhibiting the complement cascade.

## 668 **Supporting Information**

### 669 **S1 Fig: Gating strategy used to quantify transferred biotin.**

670 Gating strategy used to quantify biotin-positive amoebae. Focused cells were gated from total collected  
671 events. Next, single cells were gated, and then single amoebae were gated. Single amoebae were divided into  
672 Hoechst high and Hoechst low populations to identify images with and without human cell nuclei. Finally,  
673 biotin-positive amoebae were gated on from images with and without human cell nuclei.

### 674 **S2 Fig: Optimization of complement assay.**

675 The ability of un-supplemented human serum from different vendors to lyse amoebae was tested at various  
676 concentrations for 30 minutes, 1 hour, and 2 hours at 35°C. Samples were labeled with the viability dye  
677 Live/Dead Violet and % amoeba death was quantified using imaging flow cytometry. % amoeba death was not  
678 normalized. **(A)** Sigma Male AB Serum. Note, serum was stored at -20°C instead of -80°C. **(B)** Sigma  
679 Complement Sera Human Lyophilized Powder. **(C)** Innovative Research Pooled Normal Human Complement  
680 Serum. **(D)** Valley Biomedical Human Complement (Serum). **(E-F)** Lysis of increasing concentration of serum  
681 from Innovative Research and Valley Biomedical was tested with the addition of 150  $\mu\text{M}$   $\text{CaCl}_2$  and 150  $\mu\text{M}$   
682  $\text{MgCl}_2$  for 1 hour at 35°C.

### 683 **S3 Fig: Serum lysis assay gating strategy.**

684 Gating strategy used in the serum lysis assay. Focused cells were gated from total collected events. Next,  
685 focused events were divided into gates that either contained debris and human cells, or single amoebae. Single  
686 amoebae positive for human cells were gated and then internalization of human cells was measured. % of  
687 dead amoebae was gated from single amoebae.

### 688 **S4 Fig: Non-normalized data shown from Fig 3.**

689 Non-normalized data from the serum lysis assay shown in Figure 3. Amoebic lysis was variable and fell in to  
690 two groups, Low lysis **(A)** and **(B)** high lysis. This variability in lysis was associated with how the human serum  
691 was stored and thawed. The highest lysis was achieved with serum stored at -80°C and rapidly thawed at 37  
692 °C, leaving intact ice pellets, and then thawed to completion at room temperature. Lower lysis was achieved  
693 with serum stored at -20°C and thawed to completion at 37 °C. **(C)** Lysis from all data non- normalized. **(D)**  
694 Lysis from all data normalized to the amoeba incubated alone condition that was exposed to active human  
695 serum.

696 **S5 Fig: Internalization of human cells and amoebic death from the serum lysis assay in Fig 7.**

697 Additional data from the serum lysis assay used in Figure 7. **(A)** Internalization of human cells by vector control  
698 transfectants (open bar) or *EhROM1* (blue bar) knockdown mutants. **(B)** % of normalized amoeba death in the  
699 conditions where amoebae were incubated alone. **(C)** Non-normalized amoebic death from all conditions.

700 **S6 Fig: Gating strategy used in trogocytosis and phagocytosis assays.**

701 **(A)** Gating strategy used in the trogocytosis and phagocytosis assays shown in Figure 7. Shown are example  
702 data from a trogocytosis assay, where CMFDA-labeled amoebae were incubated with live DiD-labeled human  
703 cells. For phagocytosis assays, CMFDA-labeled amoebae were incubated with CTDR-labeled heat-killed human  
704 cells. Focused cells were gated from total collected events. Next, single cells were gated, and then single  
705 amoebae were gated. Amoebae positive for human cells were gated and internalization of human cells was  
706 measured. **(B)** Example data from a trogocytosis assay, with representative plots from the vector control  
707 condition showing internalization of human cells over time as well as representative images collected at each  
708 time point.

709

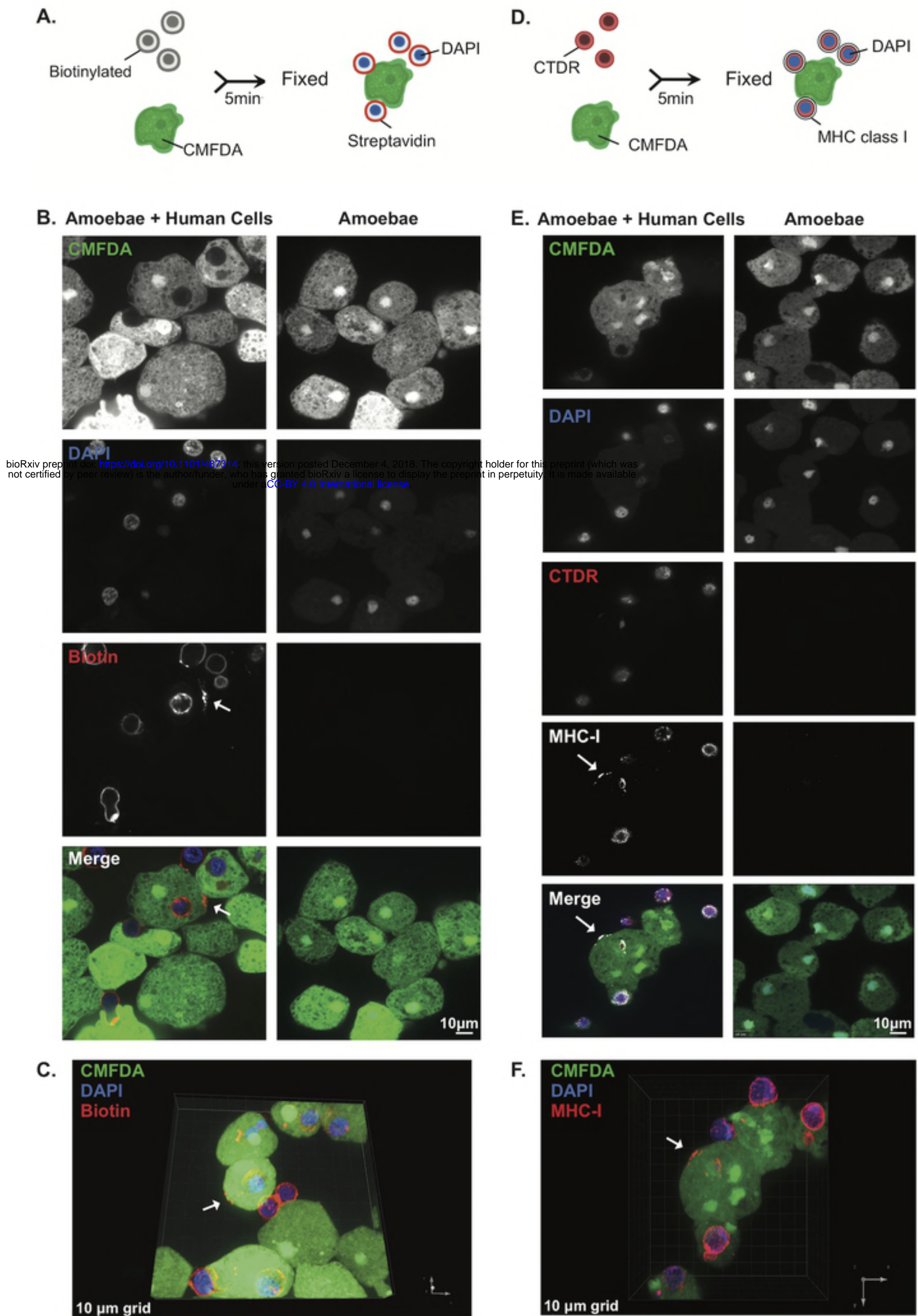
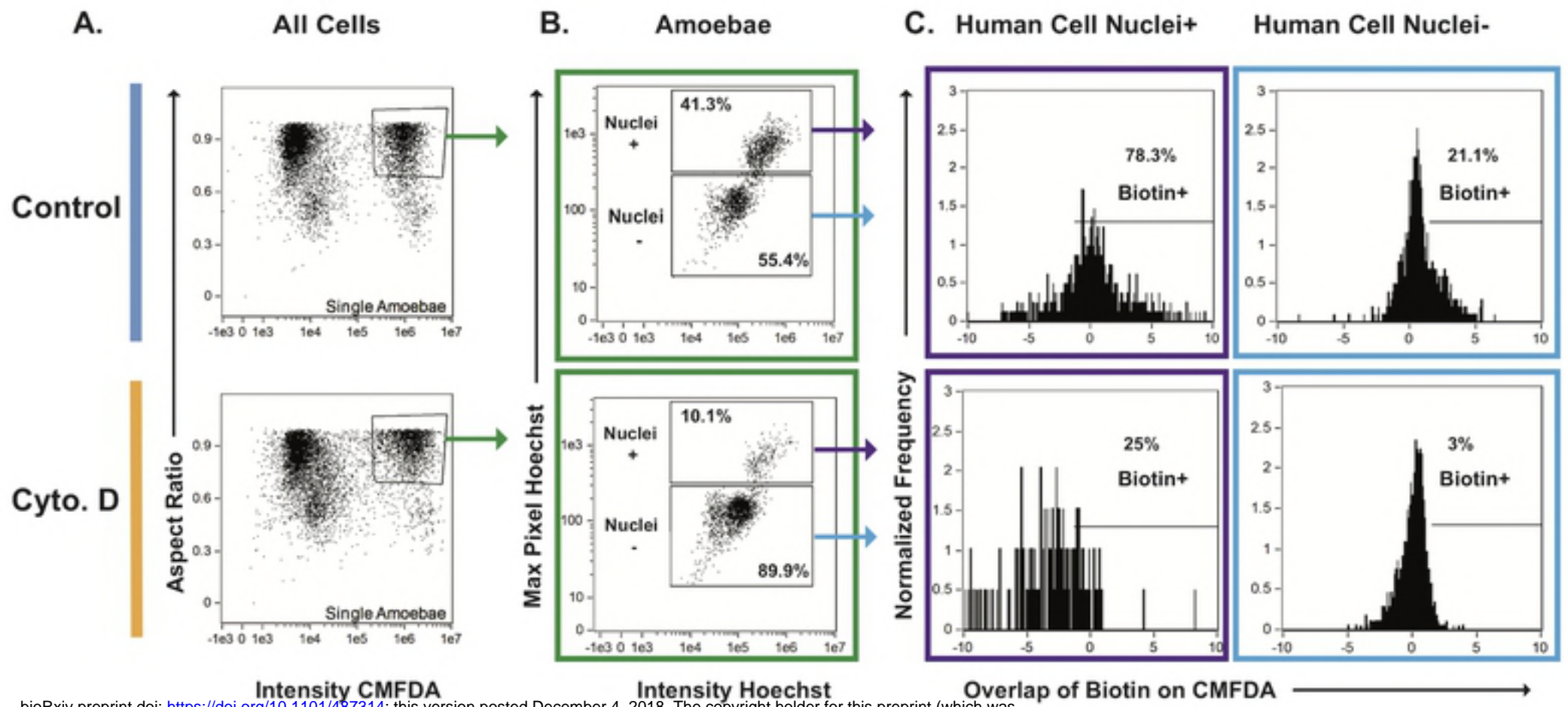


Figure 1



bioRxiv preprint doi: <https://doi.org/10.1101/487314>; this version posted December 4, 2018. The copyright holder for this preprint (which was not certified by peer review) is the author/funder, who has granted bioRxiv a license to display the preprint in perpetuity. It is made available under aCC-BY 4.0 International license.

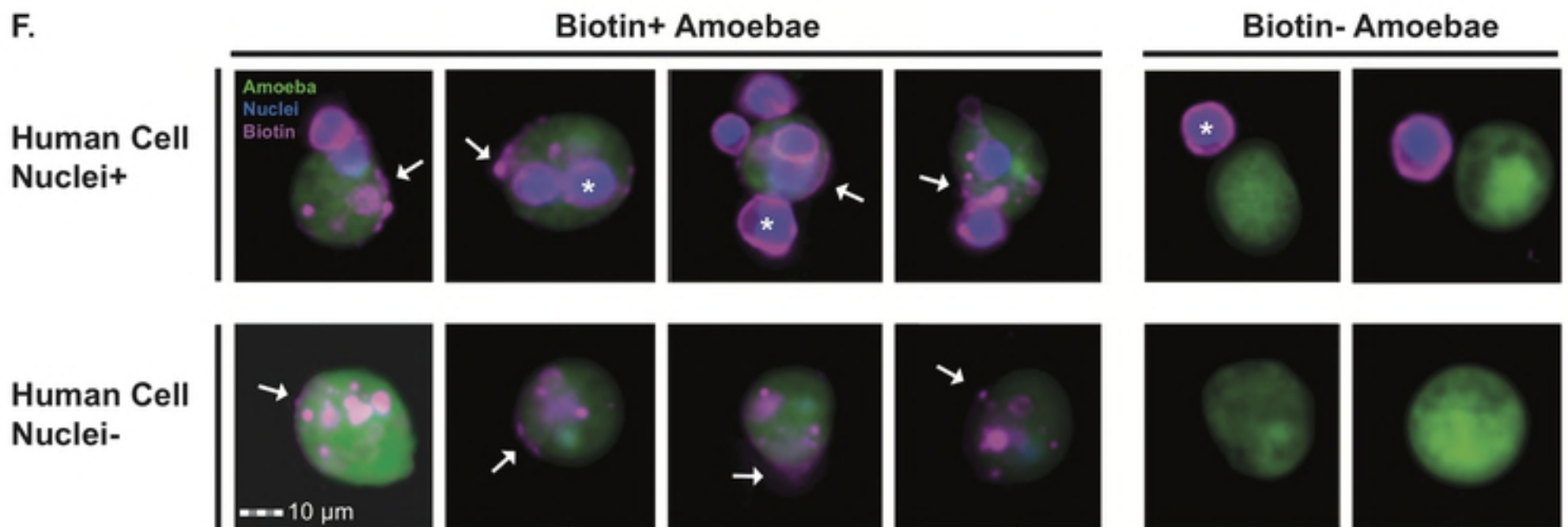
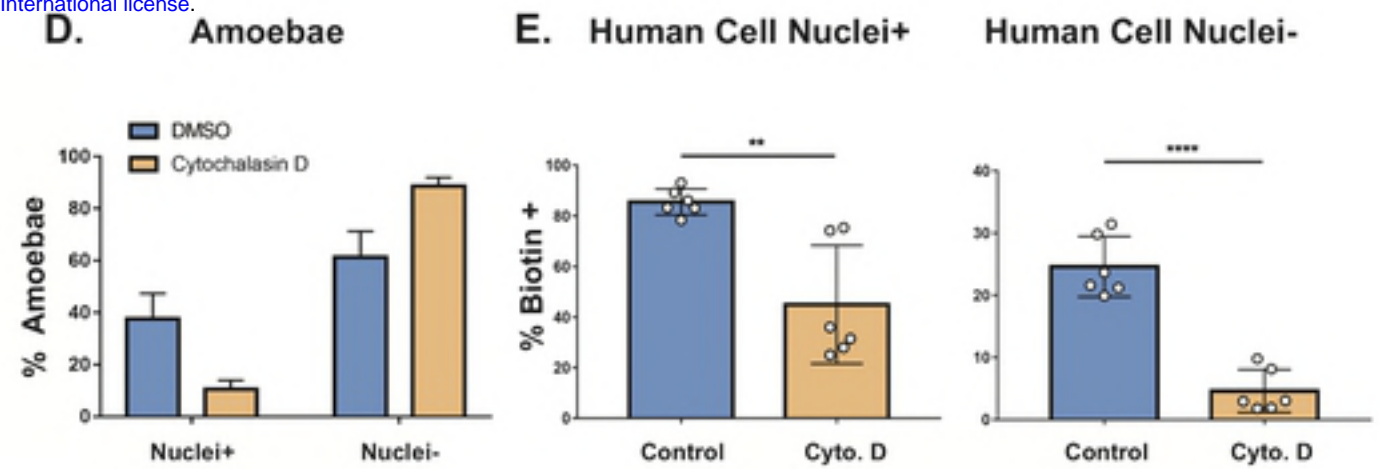


Figure 2

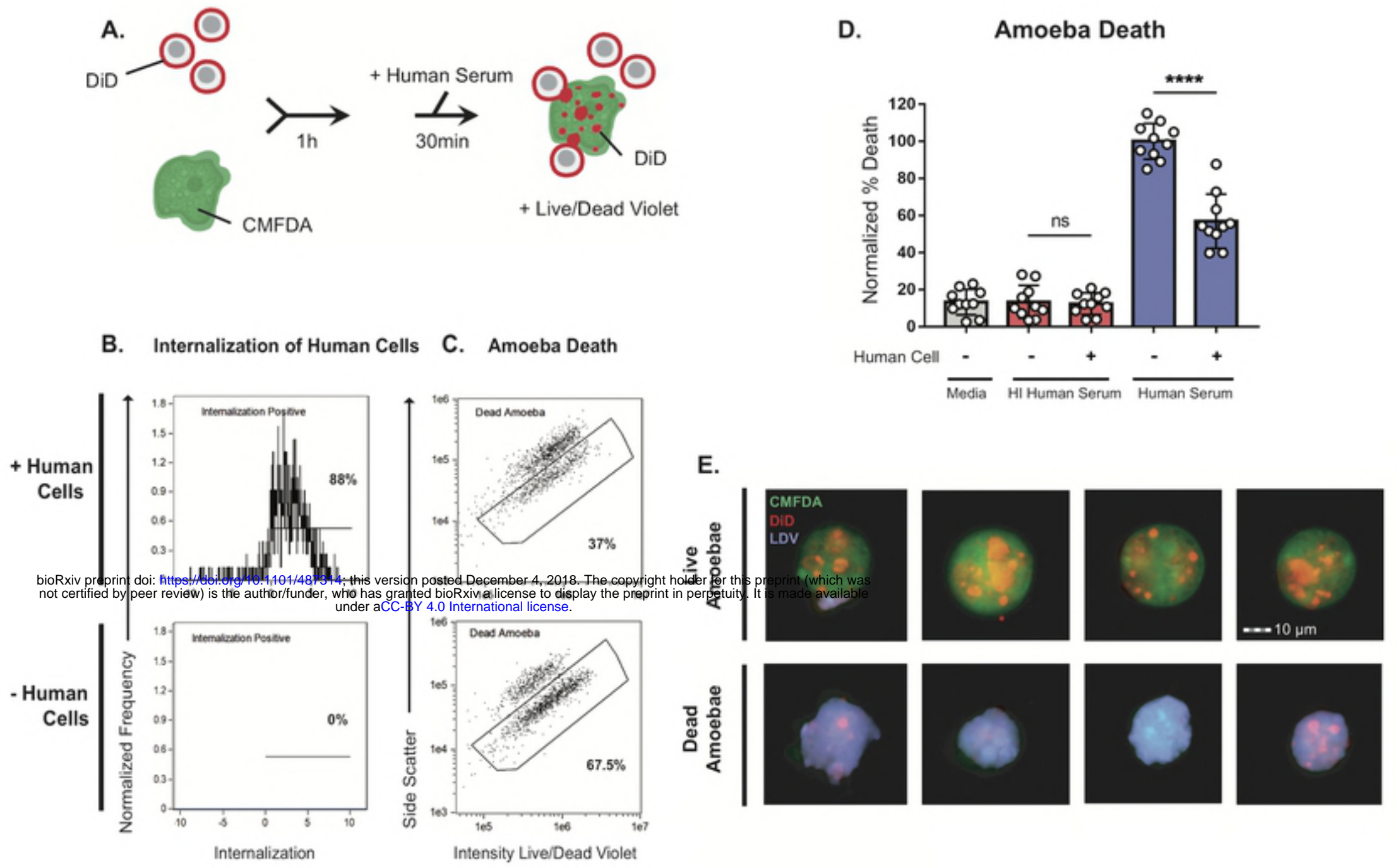
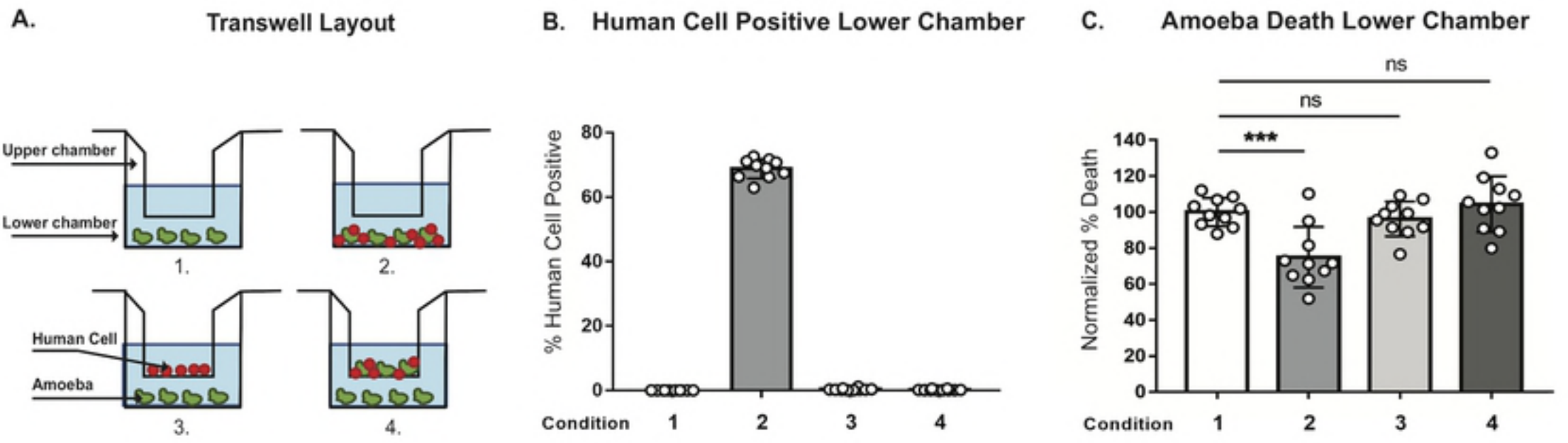
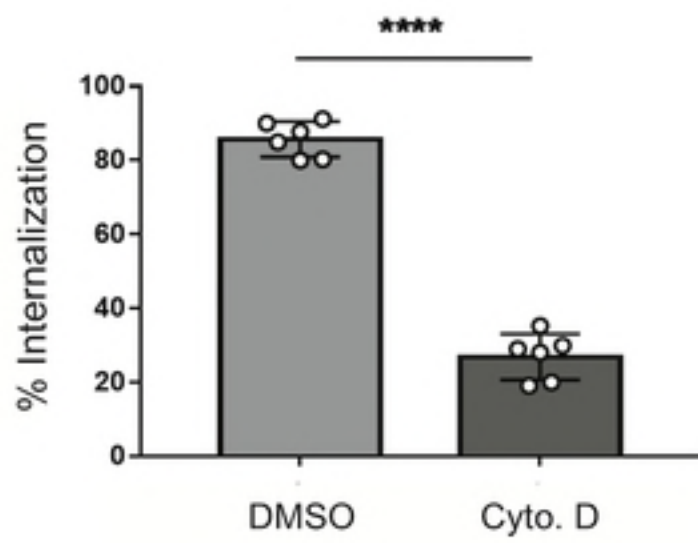


Figure 3

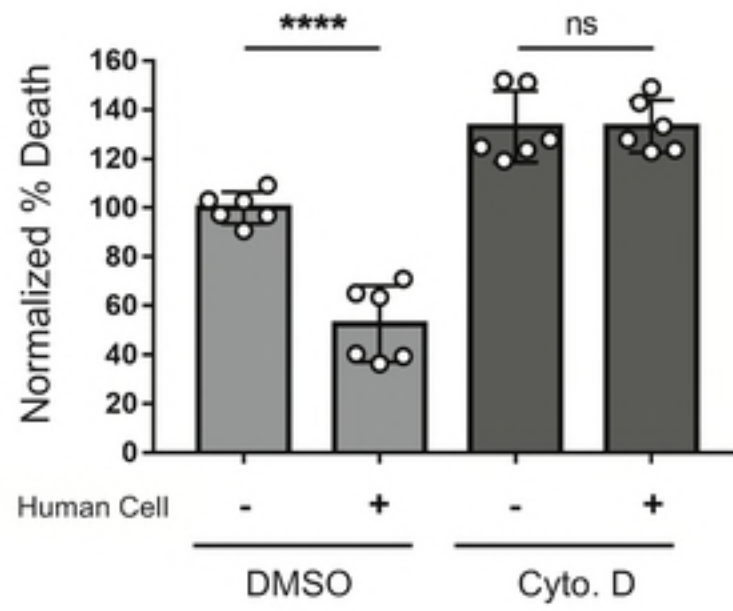


bioRxiv preprint doi: <https://doi.org/10.1101/487314>; this version posted December 4, 2018. The copyright holder for this preprint (which was not certified by peer review) is the author/funder, who has granted bioRxiv a license to display the preprint in perpetuity. It is made available under aCC-BY 4.0 International license.

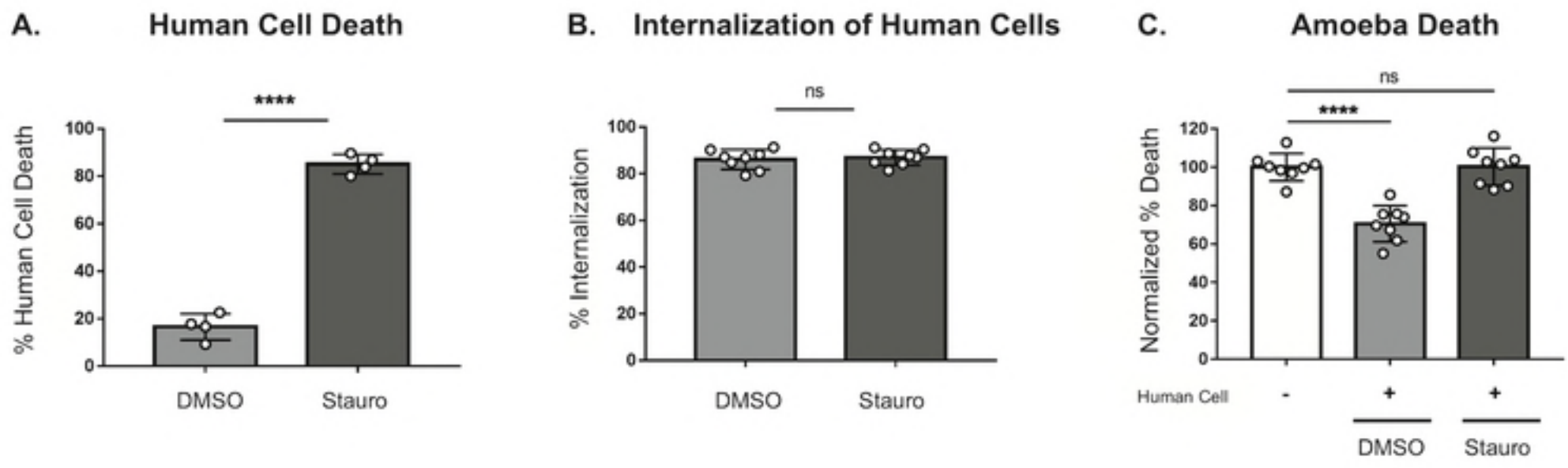
### A. Internalization of Human Cells



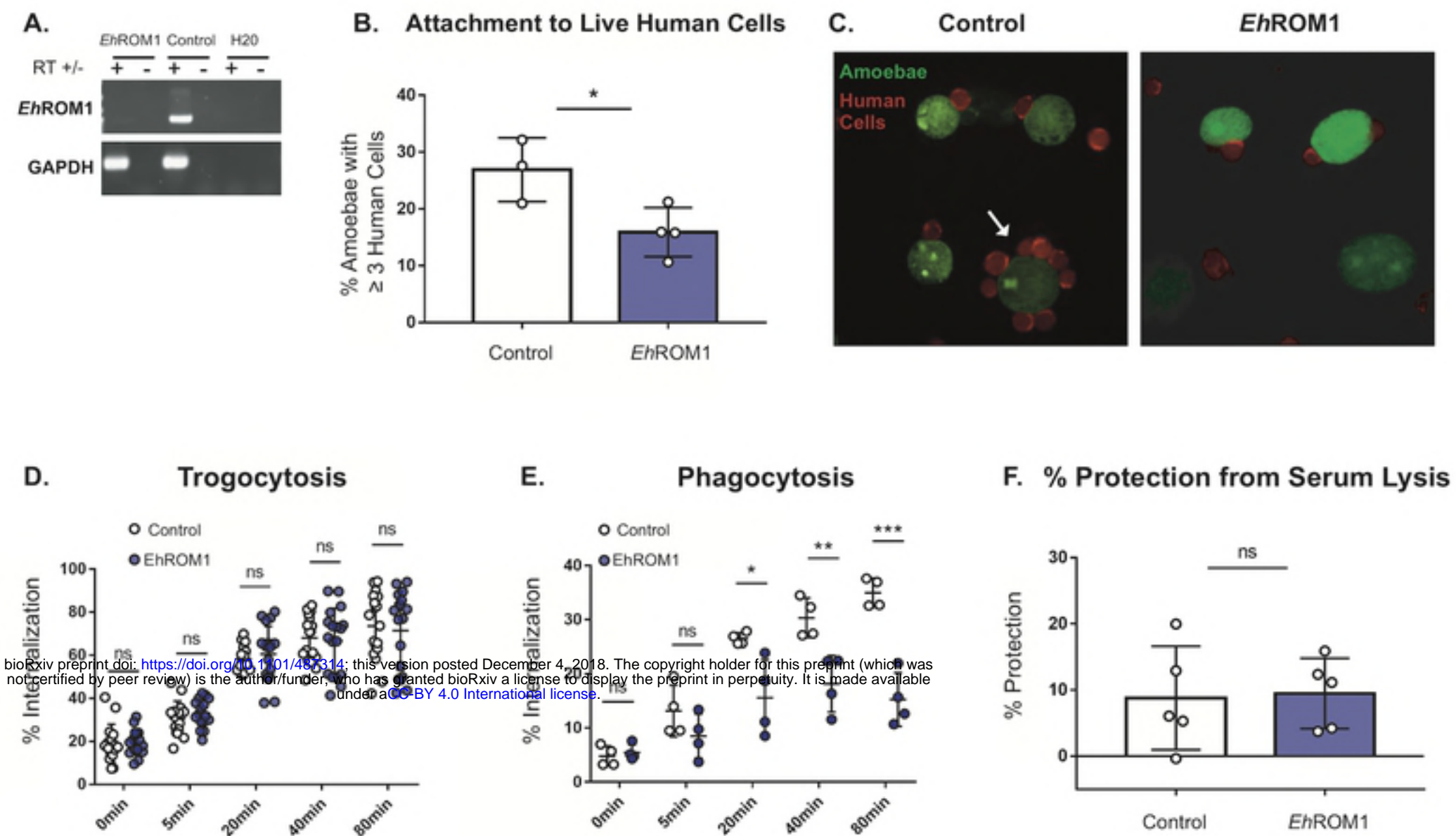
### B. Amoeba Death



bioRxiv preprint doi: <https://doi.org/10.1101/487314>; this version posted December 4, 2018. The copyright holder for this preprint (which was not certified by peer review) is the author/funder, who has granted bioRxiv a license to display the preprint in perpetuity. It is made available under aCC-BY 4.0 International license.



bioRxiv preprint doi: <https://doi.org/10.1101/487314>; this version posted December 4, 2018. The copyright holder for this preprint (which was not certified by peer review) is the author/funder, who has granted bioRxiv a license to display the preprint in perpetuity. It is made available under aCC-BY 4.0 International license.



bioRxiv preprint doi: <https://doi.org/10.1101/407314>; this version posted December 4, 2018. The copyright holder for this preprint (which was not certified by peer review) is the author/funder, who has granted bioRxiv a license to display the preprint in perpetuity. It is made available under aCC-BY 4.0 International license.

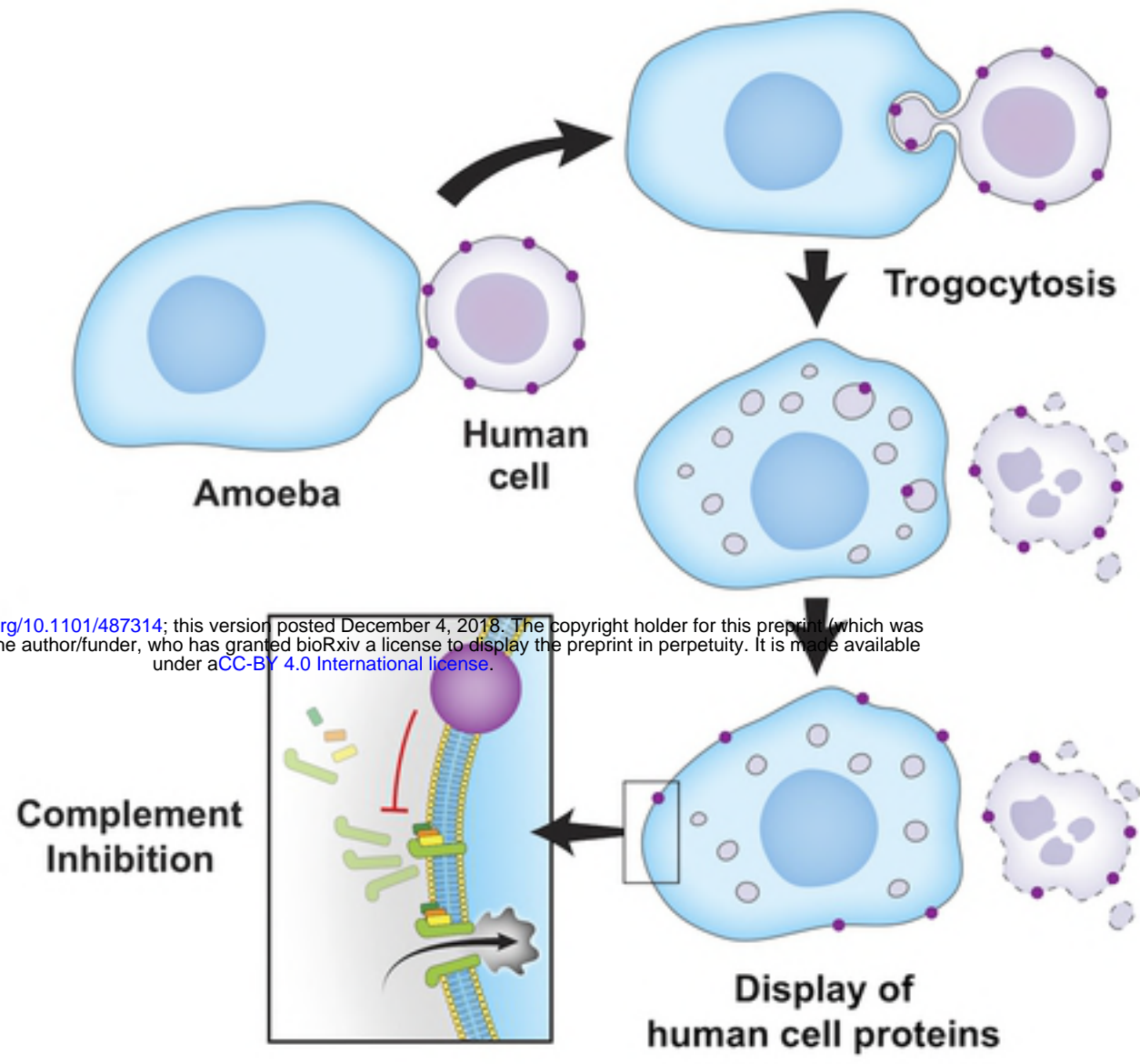


Figure 8